Journal of
MARINE RESEARCH

Volume 34, Number 2

The seasonal upwelling cycle along the eastern boundary of the North Atlantic

by Warren S. Wooster[1], Andrew Bakun[2] and Douglas R. McLain[2]

ABSTRACT

Merchant ship observations were summarized for one-degree squares along the eastern shore of the Atlantic between 7° and 44°N; monthly averages were prepared for several properties including sea surface temperature and its difference from mid-ocean values, offshore Ekman transport, and surface current. The analysis illustrates the seasonal migration of strong nearshore cooling from near Cap Vert in winter to Morocco and the Portuguese coast in summer, with a band of year-round strong cooling between 20°-25°N (near Cap Blanc). The distributions of offshore Ekman transport and temperature anomaly are in rough agreement. A seasonal response of the longshore surface current field is indicated.

1. Introduction

The climatic surface currents on the eastern sides of the major ocean basins flow slowly equatorward in broad, shallow streams. Along the coastal boundaries, at appropriate places and times of the year, upwelling of colder, nutrient-rich subsurface waters occurs. These regions are associated with high rates of primary production and with productive coastal fisheries.

Although the mechanism is incompletely understood, coastal upwelling is commonly attributed to the actions of the wind and of the rotation of the earth in

1. Rosenstiel School of Marine and Atmospheric Science, University of Miami, Florida, 33149, U.S.A.
2. Pacific Environmental Group, National Marine Fisheries Service, NOAA, Monterey, California, 93940, U.S.A.

transporting surface waters seaward and to the replacement of these waters from below. According to this simple model, the intensity of the surface winds and their direction relative to that of the coastline control the location and intensity of upwelling.

In upwelling regions, surface water temperatures are usually lower than those offshore or elsewhere along the coast. Data on sea surface temperatures and winds are routinely reported by merchant vessels; estimates of ship drift are also sometimes available. Such data can be used to examine the relations among wind stress, upwelling, and coastal currents; however, their distribution and quality is such that only climatic studies of rather crude resolution are feasible.

In an earlier study (Wooster and Sievers, 1970), maritime data from the eastern south Pacific were examined. The general pattern of seasonal variation in upwelling was identified, but the data were inadequate to establish clearly the relation between wind stress and vertical motion.

In looking at analogous circulations, it became apparent that the eastern boundary currents of the Atlantic are even more poorly known than those of the Pacific. Yet shipping patterns suggested that maritime data should be relatively abundant. Moreover, because of the development of international cooperative studies off the northwest coast of Africa, a climatological study of the region seemed desirable.

Accordingly, we have summarized available maritime data along the coasts of Europe and Africa and have examined seasonal variations in sea surface temperature and winds, and their relation to variations in coastal circulation. The region studied stretches from Spain (north of Cape Finisterre at about 43°N) to Sierra Leone (Sherbro Island at about 7.5°N), and includes the important Canary Current coastal upwelling region.

Seasonal variations in ocean conditions can also be determined from repeated oceanographic observations. These yield much more detailed and precise information, but do not necessarily represent average conditions. Such a study, based on six cruises of R. V. *Alexander von Humboldt* from 1970 to 1974, gave a seasonal picture very similar to that described below (Schemainda and Nehring, 1975).

2. Treatment of data

Wind and sea surface temperature reports for the period 1850 to 1970 were obtained from the National Climatic Center's file of marine surface observations (TDF-11). These data were checked for gross errors according to procedures described by Bakun, McLain, and Mayo (1974) and were summarized by month and by selected one-degree "square" regions.

The selection of squares used for data presentations (Fig. 1) was influenced by data abundance, which depends on the location of shipping routes. Within the total of 444 month-squares, 523,518 temperature observations were available. Most month-squares had 500 or more observations; in such squares the standard error

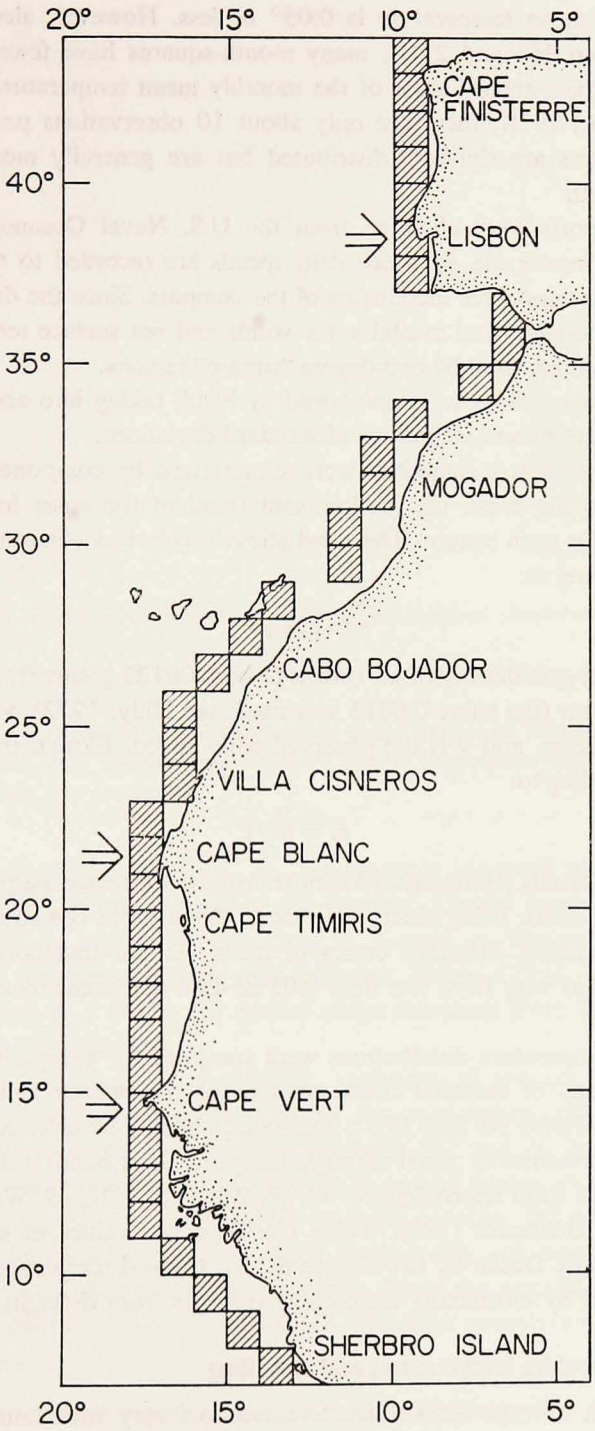

Figure 1. Location of selected one-degree squares in eastern north Atlantic. Arrows indicate location of offshore sections of Fig. 5.

of the monthly mean temperature is 0.05° or less. However, along the coast of Morocco between 35° and 27°N, many month-squares have fewer than 100 observations and the standard error of the monthly mean temperature is about 0.2°; between 30° and 29°N, there are only about 10 observations per month-square. Wind observations are similarly distributed but are generally more abundant by about five percent.

Ship drift reports were obtained from the U.S. Naval Oceanographic Office's surface current master file, in which drift speeds are recorded to tenths of a knot and directions to ten-degree increments of the compass. Since the density of reports is only about one-tenth that available for winds and sea surface temperatures, ship drift data were summarized by two-degree "square" regions.

Computed scalar values were contoured by hand, taking into account the abundance of observations and magnitude of standard deviations.

Observations of vector quantities were summarized by components parallel and perpendicular to the coast, the predominant trend of the coast having been estimated visually for each square. The wind stress vector was computed for each observation according to:

$$\vec{\tau} = \rho_a C_d v \mathbf{v}$$

where $\vec{\tau}$ is stress, ρ_a is density of air (taken to be 0.00122 g cm^{-3}), C_d is an empirical drag coefficient (the value 0.0013 was used; see Hidy, 1972), $\mathbf{v}$ is the observed wind velocity vector, and v is the observed wind speed. Ekman transport, E, was computed according to:

$$E = |\vec{\tau}|/f$$

where f is the Coriolis parameter. Ekman transport is directed perpendicular to the direction of the stress, being ninety degrees to the right of the stress vector in the Northern Hemisphere. Standard errors of mean Ekman transport (in $m^3 s^{-1}$ per meter of coastline) vary from less than 0.05 in data-rich areas to about 0.2 on the Moroccan coast.

Mid-ocean temperature distributions were compiled for comparison with coastal data. On the basis of seasonal charts of average sea surface temperatures (Min. Defense USSR, Plates 16 and 17), a mid-ocean band was selected where surface isotherms were reasonably zonal through the year. This band is 10° of longitude wide and extends from approximately 45°N, 27°W to 7°N, 49°W. Averages were calculated from Böhnecke (1936, Table III: Standard values of surface temperature of the Atlantic Ocean by two-degree fields). Coastal temperature deficit charts were constructed by subtracting the coastal averages from those in mid-ocean.

3. Average sea surface temperatures and upwelling

In mid-ocean, average sea surface temperatures vary with latitude and month

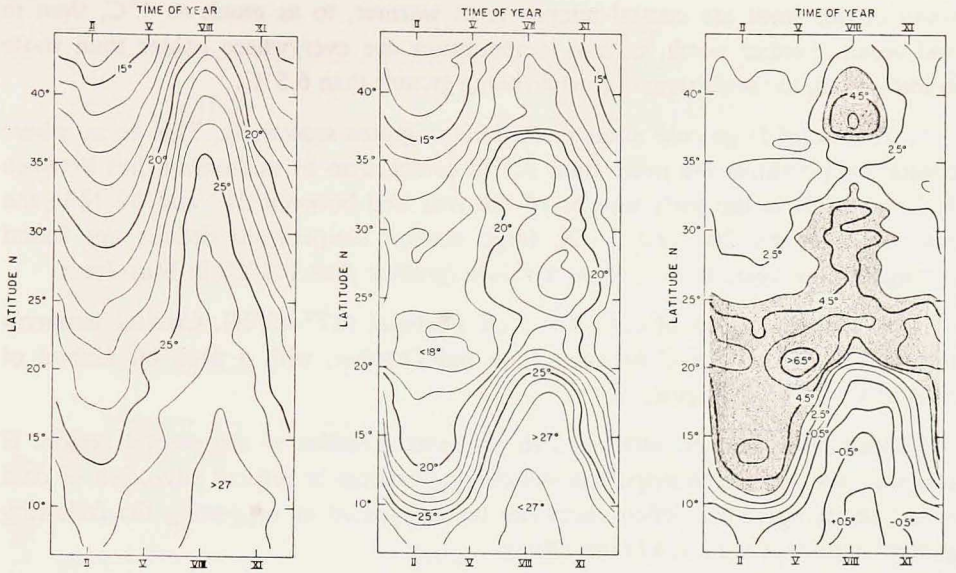

Figure 2. Monthly variation of mid-ocean average sea surface temperature (°C) in north Atlantic.

Figure 3. Monthly variation of average sea surface temperature (°C) on the eastern shore of the north Atlantic.

Figure 4. Monthly variation of coastal temperature deficit (difference between coastal and mid-ocean temperature, °C). Positive values indicate coastal temperature colder than mid-ocean; values greater than 3.5° are shaded.

in a relatively simple fashion (Fig. 2). Temperature increases smoothly, and the meridional gradient decreases, toward the equator. Lowest temperatures occur in February or March, highest temperatures in August or September. The annual range decreases equatorward from mid–latitudes; Defant (1961, Table 45) shows that for the oceans as a whole, the annual range decreases from 7.5°C at 40° latitude to 2.4°C at 10° latitude.

Along the eastern shore of the Atlantic, variations of average surface temperature follow a very different pattern (Fig. 3). An outstanding feature is the strong thermal gradient, or front, that migrates between 10° and 20°N; because of this migration, Cap Vert (at about 14° 45′N) has an annual temperature range of about 8°C. Meridional temperature minima, for example between 20° and 25°N, suggest the occurrence of coastal upwelling. Such peculiarities are more obvious in the coastal temperature deficit chart (Fig. 4) which shows the amount by which coastal temperatures differ from those in mid-ocean. The most conspicuous features in this field are the following:

a. The tropical front which moves seasonally between 10° and 20°N. Only

south of this front are coastal temperatures warmer, to as much as 1°C, than in mid-ocean. Farther north, coastal temperatures are everywhere colder than those in mid-ocean, the maximum difference being greater than 6.5°C.

b. A zone of large cold anomalies which migrates seasonally. This zone, where coastal temperatures are more than 3.5°C colder than in mid-ocean, lies between 10° and 25°N in the early months of the year and between 21° and 32°N in the summer. Between 20° and 25°N, large coastal temperature deficits are found throughout the year, with maximum values (greater than 6.5°C) in May-June.

c. A summer region of cold water off Portugal (37°-43°N). Coastal temperature deficits exceed 2.5°C between June and October, with a peak off Lisbon of more than 5.5°C in August.

These features can be attributed to processes peculiar to the coastal region. If one assumes that the principal coastal cooling process is vertical advection of cold water, the temperature deficit chart can be interpreted as suggesting the following general pattern of variation in upwelling:

12°-20°N — upwelling from January through May
20°-25°N — strong upwelling throughout the year
25°-43°N — strongest upwelling from June through October

4. Offshore extension of coastal temperature deficits

We have examined the offshore extension of sea surface temperature deficit at several selected latitudes (Fig. 5). Off Lisbon (38°-39°N) surface temperatures offshore to more than 600 km are always 1°C or more cooler than those in mid-ocean. From November through May, the temperature difference does not exceed 2.5°C, and zonal temperature gradients are small. In July through September, on the other hand, temperature differences are greater than 2.5°C even 600 km from shore; zonal temperature gradients within a few hundred kilometers of shore are much increased.

Cap Blanc (21°-22°N) is located within the zone where the coastal temperature deficit is large throughout the year. From December through July, the cold anomaly exceeds 2.5°C offshore for more than 600 km. Zonal temperature gradients are relatively large through the year. From August through November (when the tropical front is farthest north), the deficit becomes less than 2.5°C at distances greater than 300 km offshore.

Off Cap Vert (14°-15°N) the pronounced seasonality associated with the tropical front is clearly evident. During the later part of the year (June through December), zonal temperature gradients are small, and surface temperatures are within a degree of those in mid-ocean. The situation is very different from January through May,

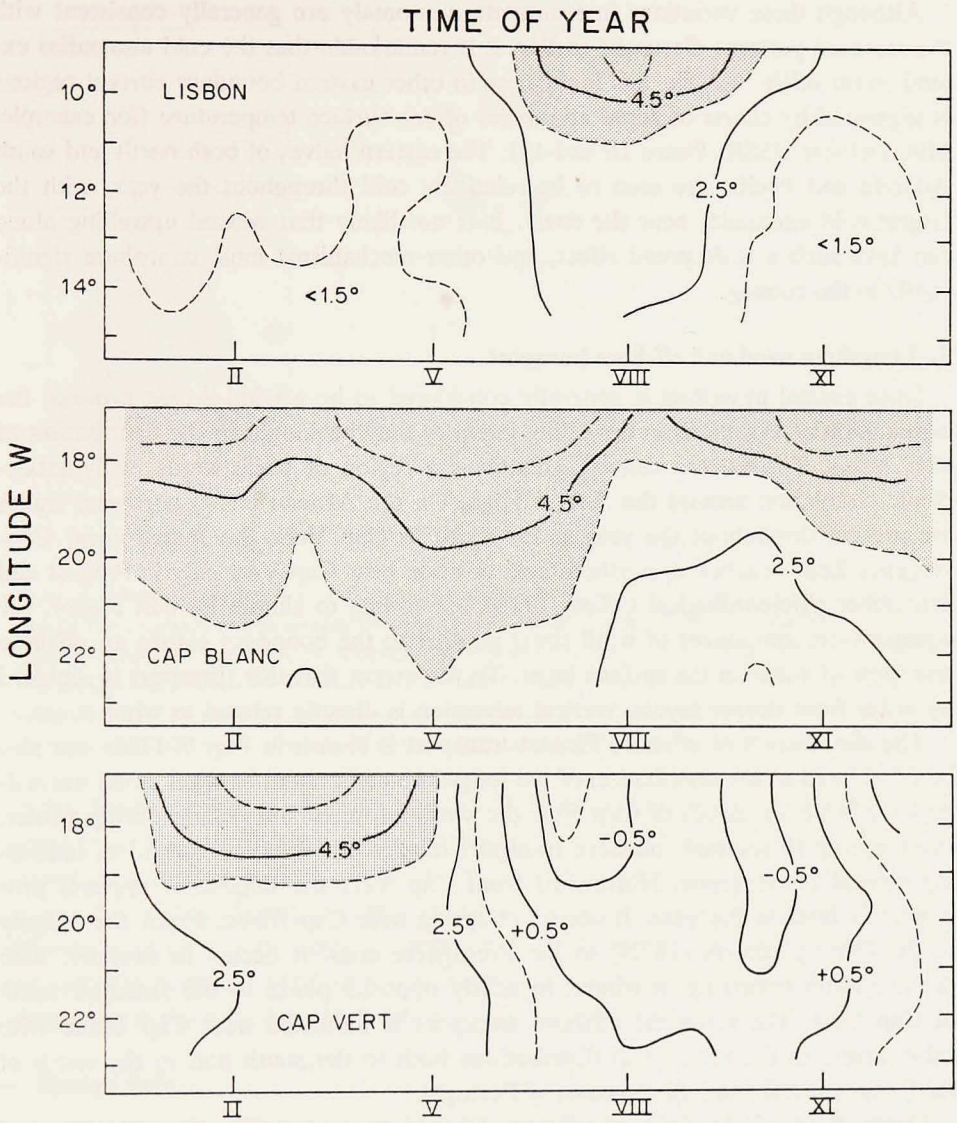

Figure 5. Monthly variation of temperature deficit (°C) in one-degree squares extending offshore from Lisbon, Cap Blanc, and Cap Vert (see Fig. 1 for location); values greater than 3.5° are shaded.

when surface waters for more than 600 km offshore are more than 2.5°C cooler than in mid–ocean, and zonal temperature gradients within a few hundred kilometers of the coast are large (in January-April, coastal temperatures are more than 4.5°C cooler than in mid-ocean).

Although these variations in temperature anomaly are generally consistent with the seasonal patterns discussed earlier, it is remarkable that the cold anomalies extend so far offshore. That this is the case in other eastern boundary current regions is suggested by charts of zonal anomalies of sea surface temperature (for example, Min. Defense USSR, Plates 16 and 17). The eastern halves of both north and south Atlantic and Pacific are seen to be relatively cold throughout the year, with the largest cold anomalies near the coast. It is not likely that coastal upwelling alone can have such a widespread effect, and other mechanisms must contribute significantly to the cooling.

5. Longshore wind and offshore transport

Since coastal upwelling is generally considered to be a wind-driven process, the explanation of variations in upwelling intensity may be sought in the distribution of wind stress. The eastern central Atlantic is a region of trade winds, with anticyclonic circulation around the Azores High. On the African coast, northeast trades are present throughout the year as far south as Cap Vert; the Intertropical Convergence Zone reaches its northernmost position near Cap Vert only in August and September (Meteorological Office, 1948). According to simple Ekman theory, the equatorward component of wind stress parallel to the boundary causes an offshore transport of water in the surface layer. To the extent that this transport is replaced by water from deeper layers, vertical advection is directly related to wind stress.

The distribution of offshore Ekman transport is shown in Fig. 6. (This can also be considered as the distribution of the longshore component of wind stress normalized for latitude). South of Cap Vert the seasonal maximum occurs during winter. From spring to summer, offshore transport relaxes and becomes negative, indicating coastal convergence. Northward from Cap Vert the maximum appears progressively later in the year. It occurs in spring near Cap Blanc. From the vicinity of the Canary Islands (28°N) to the Portuguese coast it occurs in summer, with the minimum occurring in winter, in nearly opposite phase to the situation south of Cap Vert. The strongest offshore transport is indicated near Cap Blanc with sub-maxima in the meridional distributions both to the south and to the north of the Canary Islands and off the coast of Portugal.

Comparison of the field of offshore Ekman transport (Fig. 6) with those of coastal temperature (Fig. 3) and temperature anomaly (Fig. 4) shows some similarities. The pattern of seasonal variation in the tropical temperature front which migrates past Cap Vert is quite similar to that of the southern boundary of strong offshore Ekman transport. However, the amplitude of the north-south movement seems somewhat larger in the case of the temperature.

Regions of the latitude-time diagram where coastal temperatures are several degrees cooler than those in mid ocean correspond reasonably well with regions where offshore transport is large (see for example 20°-25°N, 29°-32°N, and 37°-

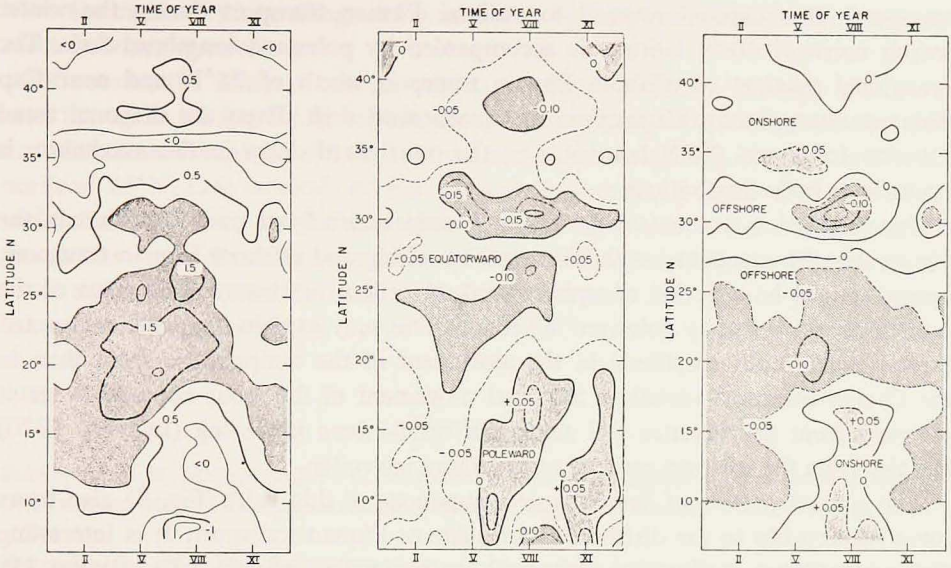

Figure 6. Monthly variation of offshore Ekman transport ($m^3 s^{-1}$ per meter of coastline) computed from longshore component of wind stress. Values greater than 1 are shaded.

Figure 7. Monthly variation of longshore component of surface current ($m\ s^{-1}$). Poleward values shaded; equatorward values greater than 0.1 $m\ s^{-1}$ hatched.

Figure 8. Monthly variation of offshore component of surface current ($m\ s^{-1}$). Onshore values greater than 0.05 $m\ s^{-1}$ shaded; offshore values greater than 0.05 $m\ s^{-1}$ hatched.

43°N). Similarly, where offshore transport has decreased, the coastal temperature deficit is usually diminished. Note, however, that between 20° and 25°N, large coastal temperature deficits continue through the last quarter of the year even though the offshore transport has decreased significantly. This as well as the phase differences of one or two months between maxima in coastal temperature deficits and offshore transport north of Cabo Bojador and off Lisbon are indications of inadequacies in distinguishing between coastal and mid-ocean processes.

6. Surface drift

Coastal upwelling and the longshore geostrophic current are linked through the redistribution of mass resulting from the nearshore accumulation of denser upwelled water and the transport offshore of lighter surface water (Sverdrup, Johnson and Fleming, 1942, p. 501). The balance between the resulting pressure gradient and the Coriolis force produces an equatorward geostrophic current in the equilibrium state.

The seasonal field of longshore flow (Fig. 7) shows some correspondence with major features of the offshore Ekman transport (Fig. 6). Off the coast of Portugal the maximum equatorward flow corresponds to the period of maximum offshore

transport. The seasonal reversal to onshore Ekman transport during the winter season north of 40°N latitude is accompanied by poleward longshore flow. The meridional maxima of offshore Ekman transport north of 28°N and near Cap Blanc are associated with maxima in equatorward drift. Even the diagonal trend between 15°N and 25°N latitude, i.e., the, northward delay in the maximum, is common to both distributions.

Equatorward movement of the tropical temperature front past Cap Vert in the winter (Fig. 3), associated with enhanced upwelling and offshore Ekman transport, is seen also to be a period of equatorward advection; northward movement of the front is accompanied by poleward advection. This may explain the previously noted greater north-south amplitude in the movement of the temperature front than in the Ekman transport variation. Seasonal movement of the front appears to result not only from the advance and retreat of wind-driven upwelling (Ingham, 1970) but also from the seasonal reversal of longshore advection.

The general pattern of the offshore component of ship drift (Fig. 8) also bears some relationship to the distribution of offshore Ekman transport. It is interesting to note that there is always a slight onshore component of ship drift between 33° and 38°N even where offshore Ekman transport is positive. This discrepancy may arise because ship drift takes place in the upper part of the Ekman layer where motion is closer to the direction of the wind stress; ships are driven toward shore by the prevailing onshore component of the wind stress in this region. It is also noteworthy that in the 20°-25°N band of permanent coastal temperature deficit, the offshore component of ship drift is positive throughout the year.

7. Summary

The analysis of sea surface temperature data shows that coastal temperatures along the eastern shore of the north Atlantic are nearly everywhere lower than those in mid-ocean, often by more than 2.5°C.Only south of a strong thermal front that migrates seasonally between 10° and 20°N past Cap Vert are coastal temperatures higher than those in mid-ocean. North of the front, a zone of large cold anomalies extends from 10° to 25°N in the early months of the year and from 21° to 32°N in summer, when relatively cold water is also observed off Portugal. Between 20° and 25°N, large coastal temperature deficits occur throughout the year.

Surface winds are the major driving force for coastal processes, and the distribution of offshore Ekman transport computed from wind stress shows a strong resemblance to that of coastal temperature deficit, with large cold anomalies being associated with large values of offshore transport. Although available surface current data are crude, the patterns of longshore and offshore components are also clearly consistent with those of offshore Ekman transport and coastal temperature deficit. Thus all of the data fit with the simple hypothesis that low coastal tempera-

tures are caused by upwelling which is driven by longshore wind stress, as is the coastal surface circulation.

Of course, the analysis relates only to average conditions in large areas, and even there it is inadequate to explain the offshore extension of the coastal temperature deficit or the phase differences between wind stress and temperature deficit north of 25°N. Our methods do not succeed in completely separating coastal and mid-ocean processes, nor do they allow for non-linearities in these processes. Yet the results are sufficiently promising to suggest that maritime data from specific years and regions could be used to elucidate seasonal and year-to-year variations in eastern boundary regimes.

REFERENCES

Bakun, A., D. R. McLain, and F. V. Mayo. 1974. The mean annual cycle of coastal upwelling off western North America as observed from surface measurements. Fish. Bull., *72:* p. 843–844.

Bohnecke, G. 1936. Das Beobachtungsmaterial und seine Aufbereitung, *in* Wissenschaftliche Ergebnisse der Deutschen Atlantischen Expedition auf dem Forschunge-und Messungsschiff "Meteor" 1925–1927, v. 5, part 1: p. 1–186.

Defant, A. 1961. Physical Oceanography. London: Pergamon, v. 1, 729 pp.

Hidy, G. M. 1972. A view of recent air-sea interaction research. Bull. Amer. Meteorol. Soc., *53:* p. 1083–1102.

Ingham, M. C. 1970. Wind and sea-surface temperature off Mauritania, Sierra Leone. J. Mar. Tech. Soc., *4:* p. 55–57.

Meteorological Office. 1948. Monthly meteorological charts of the Atlantic Ocean. Air Min. Meteorol. Off. No. 483.

Ministry of Defense USSR. 1953. Morskoi Atlas. v. 2.

Schemainda, R. and D. Nehring. 1975. The annual cycle of the space-temporal dislocation of the North-West African upwelling region. Unpublished paper presented at Third International Symposium on Upwelling Ecosystems, Kiel, Fed. Rep. Germany, 25–28 Aug. 1975.

Sverdrup, H. U., M. W. Johnson, and R. H. Fleming. 1942. The Oceans: their physics, chemistry, and general biology. New York: Prentice-Hall. 1087 pp.

Wooster, W. S. and H. Sievers. 1970. Seasonal variations of temperature, drift and heat exchange in surface waters off the west coast of South America. Limnol. Oceanogr., *15:* p. 595–605.

Received: *8 September, 1975;* revised: *19 January, 1976.*